Egyptian Journal of Chemistry

Design, synthesis, characterization, and biological evaluation of new diazole- benzamide derivatives as glucokinase activators with antihyperglycemic activity

Ammar A. Hamid[1], Omar F. Abdul-Rasheed[2], Monther F. Mahdi[3], Abdul-Jabbar Atia[4]*

[1]*Department of Pharmaceutical Chemistry, College of pharmacy, University of Kerbala, Iraq;*
[2]*Department of Chemistry and Biochemistry, College of Medicine, Al-Nahrain University, Iraq;*
[3]*Department of Pharmaceutical Chemistry, College of Pharmacy, Mustansiriyah University, Iraq;*
[4]*Department of Chemistry, College of Science, Mustansiriyah University Iraq*

Abstract

Background: Glucokinase (GK) is an essential enzyme that acts as an insulin sensor and is involved in glucose regulation. It's present in pancreatic β -cells and hepatocytes in the liver. As a result, GK might be a promising target for treating T2DM. GK activators are new antihyperglycemic drug candidates that work by activating the enzyme allosterically. **Methodology:** New benzamide nucleus derivatives were carefully developed, subjected to energy minimization, and then docked utilizing the Genetic Optimization of Ligand Docking method (GOLD). Following the in silico design and docking process, chemical syntheses utilizing a well-defined synthetic strategy culminated in the successful syntheses of these compounds, which were purified and characterized. A reliable animal model for T2DM was obtained by feeding mice with high fructose diet for 8 weeks. These mice were used then to study the hypoglycemic effect of the synthesized compounds by the application of OGTT. Finally an enzymatic assay was done to evaluate the activation of these compounds to the target enzyme. **Results:** The docking studies of the synthesized compounds (1c & 2c) revealed a complementary fit in the GK protein's allosteric binding site. Considering the PLP fitness, the hydrogen bonding and the hydrophobic interactions; compound 2c was superior to compound 1c. All the compounds were synthesized with a good yield. Characterization and identification of these compounds were done individually using FT-IR spectroscopy, ^{1}H & ^{13}C NMR and MS. The results of these analyses were in consistence with the proposed structures of the compounds. The animal model was successfully achieved, this was confirmed by the resultant impaired OGTT and the observation of the metabolic changes that occurred after fructose feeding period. *In vivo* biological evaluation using OGTT revealed a good glucose lowering activity of the synthesized compounds. These results were compatible with that obtained from *in vivo* enzymatic activity assay and *in silico* studies which showed that compound 2c has better activity than compound 1c. These novel benzamide derivatives could be employed as a starting point for developing safe, effective, and orally accessible GKAs to treat T2DM.

1. Introduction

D.M. is a long-term metabolic disease that causes disturbed glucose and lipid metabolism. It results from deficiency of insulin secretion or poor insulin sensitivity [1]. The most common kind of diabetes is T2DM, which accounts for 90-95 percent of all cases worldwide. [2]. It is characterized by poor insulin sensitivity and the incidence of hyperinsulinemia [3]. The long term hyperglycemia results in vascular complications (coronary artery diseases, stroke, nephropathy, neuropathy and retinopathy) [4].

The phosphorylation of glucose to glucose-6-phosphate is catalyzed by GK (ATP: D- glucose 6-phosphotransferase, EC 2.7.1.2) [5]. The human type of GK has low affinity for glucose that its Km value; the concentration of the substrate at which half of the maximum enzyme activity is achieved, is about 8 mM [6].

Glucokinase is expressed primarily in hepatocytes and pancreatic β- cells, wherein both of the intracellular and extracellular levels of glucose levels are almost the same (≤ K_m value) [7].

_____

Therefore, any change in the plasma concentration of glucose leads to a prominent and direct change in the glucokinase activity. By this, GK has a unique effect in blood glucose regulation. [8]

GK contains an allosteric activator site that results in a higher catalytic rate (Kcat) and a lower glucose Km. Glucokinase activators (GKAs) work by binding to this activator site. Because of their impact on pancreatic islets and liver hexokinase, GKAs promote insulin secretion and glucose uptake by the liver in vivo, making them potentially promising therapeutic agents for the treatment of diabetes. [9]&[10].

The fundamental functions of GK in hepatocytes and β-cells are primarily dissimilar but complementary, therefore, the therapeutic effect of GKAs in these organs are also dissimilar.

GK has a regulatory effect in glucose metabolism of pancreatic β-cells (glycolysis and oxidation) providing that even little changes in enzyme activity (by ∼ 10 – 20 %), have a noticeable impact on glucose metabolism [11]. On the other hand, as the first stage in glycogen production, the enzyme sustains the high capacity process of glucose clearance in the liver from postprandial portal circulation.

In a few words, GK serves as a sensor molecule for glucose, while the GK-containing cells serves as a sensor cells for glucose concerned in sensing process for glucose level [12].

The discovered GKAs can be classified chemically to the following groups:
1- Model with carbon in the center (alkanes, alkenes and cyclopropyl subtypes).
2- Model with an aromatic ring in the center.
3- Model based on amino acids.
4- Model based on nitrogen.

SAR (structure activity relationship) studies using crystallography for different series of GKAs revealed the importance of the molecular recognition interacting moiety necessary for binding of these ligands to the enzyme's allosteric activator binding location. These interacting moieties can be simplified as follow [13]:

- R1 aryl moiety provides hydrophobic interactions (or $\pi - \pi$ attraction) with Tyrosine 214 and Tyrosine 215 residues.
- R2 interacts hydrophobically with the Methionine 235 side chain.
- R3 provides H-bond donor/acceptor attraction with the Arginine 63 carbonyl and amide NH (fig.1).

GKA derivatives had been found and patented in considerable numbers. Their mechanisms of action at molecular, cellular, and organ levels had been well established and explained in details. The results indicated that the biological and medical bases on which GKAs are based are valid, and that they are a promising new class of antidiabetic therapy for normalizing hyperglycemia in patients with T2DM without medically significant side effects, with the

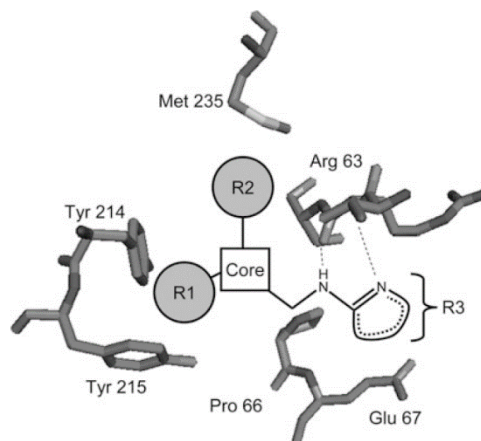exception of moderate hypoglycemia at high drug doses.

Figure 1: molecular recognition interactions between GKA pharmacophores with the corresponding allosteric activator binding sites.[14]

This work aimed to:
1. Design, synthesize, and characterize new diazole benzamide derivatives, as glucokinase activators and assessing their biological activity and properties in silico using modern docking software supplied by Cambridge Crystallographic Data Center.
2. Design of diabetic animal model by inducing hyperglycemic changes in mice by high-fructose diet.
3. In vivo evaluation of the synthesized compounds by achieving oral glucose tolerance test on the modeled mice.
4. Enzymatic activity evaluation of the synthesized compounds using glucokinase activity kit.

Materials & Methods
Materials: The materials consumed in this work are listed in the table (1).
Instruments:
The instruments used in this research are listed in the table (2).
Methods:
In silico docking studies:
Energy minimization:
Both protein and ligand energies were minimized using Chem3D and Mercury (version 4.1.0), then The PDB format was used to save the energy-minimized protein, while the mol2 format was used to save the energy-minimized ligand.
Preparation of ligand and protein receptor:
The GK enzyme crystal structure (PDB ID: 5V4X) was downloaded from the Protein Data Bank. (Figure 2). All water molecules and metals of this protein were removed and hydrogen atoms were added to obtain the correct ionization and tautomerization of amino acid residues [15].

_____

_____

Table (1): The materials consumed in this study, their manufacturing companies and country of origin.

No.	Material	Manufacturer	Country	Purity %
1	Aniline	Merck	Germany	99.5
2	5-amino-1H-imidazole-4-carbonitrile	Hangzhou Hyper Chem	China	95.0
3	Chloroform	Merk	Germany	99.5
4	3-(Chlorosulfonyl) benzoic acid	Sigma-Aldrich	USA	95.0
5	D (-)-Fructose powder	Scharlau	Spain	98..5
6	Dimethyl sulfoxide (DMSO)	Scharlau	Spain	99.9
7	Ethanol	BDH	England	99.0
8	Hexokinase Microplate Assay Kit	MyBioSource	USA	------
9	Metformin HCl tab.	Merck Serono	France	------
10	Silica gel GF254(type 60) aluminum plates	Merk	Germany	99.0
11	Thionyl chloride (SOCl2)	alpha chemika	India	97.0

Table (2) the instruments used in this study, their manufacturing companies and country of origin.

| No.	Instrument	Manufacturer	Country
1	Accu-Chek Active Glucometer kit	Roche	Germany
2	Centrifuge	Hettich Zentrifugen	Germany
3	Chiller Julabo VC (F30)	GMBH	Germany
4	Electronic melting point apparatus	Electro thermal 9300	USA
5	FT-IR spectrophotometer	Schimadzu	Japan
6	^{1}H, ^{13}C-NMR spectrophotometer	Bruker	Germany
7	Mass spectrometer	Schimadzu	Japan
8	Microplate reader (GloMax® Discover)	Promega	USA
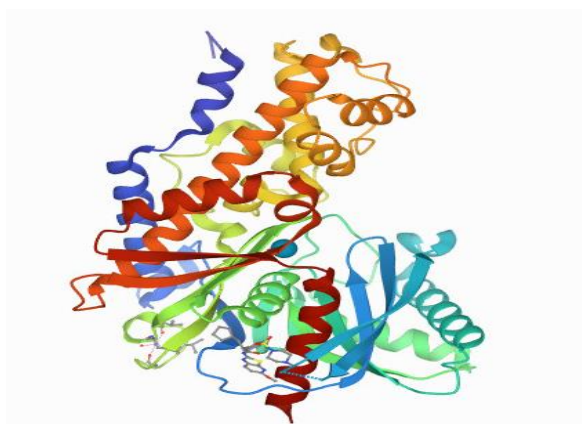
Figure (2): Crystal structure of human glucokinase complexed with a synthetic activator
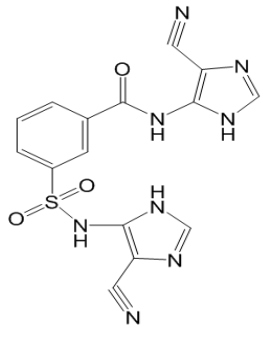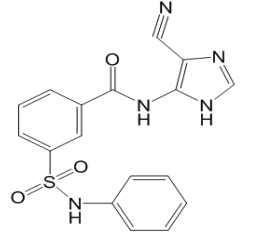
Docking procedure

Molecular docking was performed using the full licensed version of GOLD (*v.* 5.7.1). Receptors were set up for docking process using the Hermes visualizer software and the GOLD suite. The binding sites used for docking process were identified by detecting all the protein residues within 10 Å distance away from the reference ligand that exist originally with the downloaded protein structures complex [16].

Chem PLP (Piecewise Linear Potential) was utilized as a scoring function. The conformation of the docked molecule with the greatest GOLD score (fitness) was chosen, and the mode of binding was studied sequentially, according to Chem PLP. After GOLD running was finished, the solutions were saved to study and evaluate the predicted interaction and forces between the amino acid residues of GK protein (binding sites) and the functional groups of the candidate ligands [17] .

Depending on the docking results, two compounds were selected to be synthesized; these compounds were listed in table (3) below with their structures and IUPAC names.

_____

Table (3): structures of the designed compounds:

Compound	Structure	IUPAC name
1c		N-(4-cyano-1H-imidazol-5-yl)-3-(N-(4-cyano-1H-imidazol-5-yl)sulfamoyl) benzamide
2c		N-(4-cyano-1H-imidazol-5-yl)-3-(N-phenylsulfamoyl) benzamide

Chemical synthetic methods

The synthesis of the diazole benzamide derivatives was achieved following procedures listed below and steps were summarized in (scheme 1) [18] & [19].

Synthesis of compound (1a): 3-(N-(4-cyano-1H-imidazol-5-yl) sulfamoyl) benzoic acid

Dry 3-(chlorosulphonyl) benzoic acid (2.2 g, 0.01 mol) in (25 ml) chloroform was placed in a round bottomed flask 100 ml in size, fitted with a stirring bar and condenser, stirred and refluxed to (70 ºC). After 15 minutes, (1.08 g, 0.01 mol) of 5-amino-1H-imidazole-4-carbonitrile (aromatic amine) was added to the mixture, which was then refluxed for 7 hours (until the reaction was complete as determined by TLC). The flask's contents were cooled to room temperature, then filtered, washed and dried to obtain the precipitate of benzoic acid sulphonamide (compound 1a).

Synthesis of compound (1b): 3-(N-(4-cyano-1H-imidazol-5-yl)sulfamoyl) benzoyl chloride

Compound (1a) (2.92 g, 0.01 mol) was dissolved in 25 ml chloroform, stirred for 15 minutes, then (0.73 ml, 0.01 mol) of thionyl chloride was added to the solution and refluxed for 4 hours. The solvent was evaporated by rotary evaporator after the reflux was completed, and the result was filtered, then recrystallized by ethanol, dried, and collected as compound (1b).

Synthesis of compound (1c): N-(4-cyano-1H-imidazol-5-yl)-3-(N-(4-cyano-1H-imidazol-5-yl)sulfamoyl) benzamide.
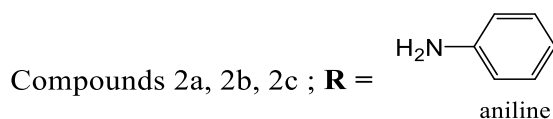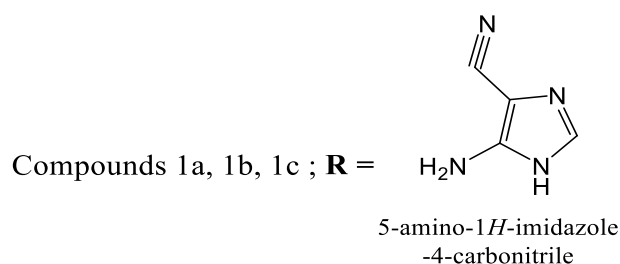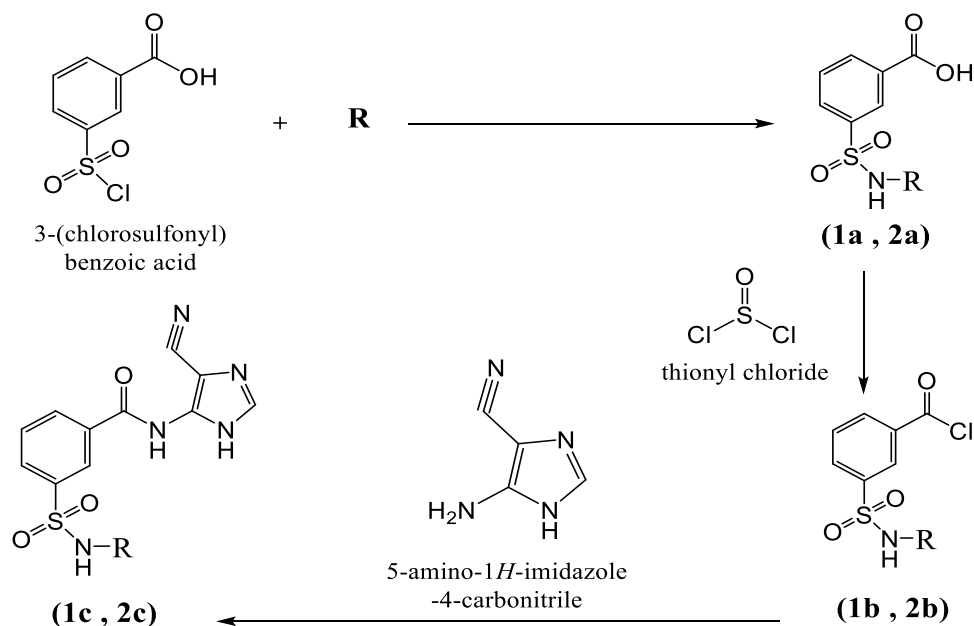
The benzoyl chloride (compound 1b) (3.11 g, 0.01 mol) was refluxed with the diazole amine (5-amino-1H-imidazole-4-carbonitrile) (1.08 g, 0.01 mol) in 30 ml chloroform for 7 hours and the final product compound (1c) was received after the evaporation of chloroform and recrystallization from ethanol to get the final pure product.

Synthesis of compound (2a): 3-(N-phenylsulfamoyl) benzoic acid

Dry 3-(chlorosulphonyl) benzoic acid (2.2 g, 0.01 mol) in (25 ml) chloroform was placed in a round bottomed flask 100 ml in size, fitted with a stirring bar and condenser, stirred and refluxed to (70 ºC). After 15 minutes, 0.93 g (0.01 mol) aniline (aromatic amine) was added to the mixture, which was then refluxed for 7 hours (until the reaction was complete as determined by TLC). To obtain the precipitate of benzoic acid sulphonamide, the contents of the flask were cooled to room temperature, then filtered, washed, and dried (compound 2a).

Synthesis of compound (2b): 3-(N-phenylsulfamoyl) benzoyl chloride

Compound (2a) (2.77 g, 0.01 mol) was dissolved in 25 ml chloroform, mixed for 15 minutes, and then added to the solution (0.73 ml, 0.01 mol) of thionyl chloride and refluxed for 4 hours. The solvent was evaporated by rotary evaporator after the reflux was completed, and the result was filtered, then recrystallized by ethanol, dried, and collected as compound (2b).

_____

3-(chlorosulfonyl) benzoic acid

+ **R**

(1a , 2a)

thionyl chloride

(1c , 2c)

5-amino-1*H*-imidazole -4-carbonitrile

(1b , 2b)

Compounds 1a, 1b, 1c ; **R =**

5-amino-1*H*-imidazole -4-carbonitrile

Compounds 2a, 2b, 2c ; **R =**

aniline

Scheme (1): General synthetic pathway of compounds (1c, 2c)

2.4.12 Synthesis of compound (2c): N-(4-cyano-1H-imidazol-5-yl)-3-(N-phenylsulfamoyl) benzamide.

The benzoyl chloride (compound 2b) (2.96 g, 0.01 mol) was refluxed with the diazole amine (5-amino-1H-imidazole-4-carbonitrile) (1.08 g, 0.01 mol) in 30 ml chloroform for 7 hours and the final product compound (2c) was received after the evaporation of chloroform and recrystallization from ethanol to get the final pure product.

Methods of characterization and identification
Thin layer chromatography (TLC)

The ascending Thin Layer Chromatography was performed on E. Merck (Germany) Kieslgel GF254 (60) aluminum plates to assess the purity of the synthesized compounds and observe the reaction progress. Compounds were viewed by the exposure to UV$_{254}$ light [20].
The following solvent system was used to elute the chromatogram: Benzene: Ethyl acetate (70: 30) [21].

Melting points

The melting points of the synthesized compounds and their precursors were accomplished out using the electronic melting point apparatus (digital Stuart scientific SMP30) and are uncorrected.

Infrared spectra:

Determinations of infrared spectra were done and recorded using Shimadzu FTIR-8400 (with resolution; 4[1/cm] and no. of scans; 15) at the chemistry department / College of Science / Mustansiriyah University.

_____

^{1}H & ^{13}C-Nuclear Magnetic Resonance (^{1}H & ^{13}C-NMR)

The ^{1}H & ^{13}C-NMR spectra were recorded for the final synthesized compounds; (1c & 2c) using Bruker DMX-500 NMR spectrophotometer (300 MHZ, solvent DMSO-d$_6$) with TMS (tetramethylsilane) as an internal standard reference at Sharif University of Technology / Iran.

Mass spectroscopy

Mass spectroscopy was done for the final products; compounds (1c & 2c) using mass spectrometer (Varian 3900, 5793 Network Mass Selective Detector) / Tehran University / Iran.

Animal model design:
Animals:

50 male albino laboratory mice (8 weeks aged and 25-30 g wieghed) were purchased from National Center for Drug Control and Research (NCDCR) and kept in controled room teperature (~ 22 ℃) on a normal 12 hour light/ dark cycle. Soon after arrival of the animals, their indivdual weights were recorded and an initial OGTTs were done for them separately.

For an 8-week period, all of the mice were allocated to one experimental group and given free access to the rodents' chow (ad libitum) and drinking water supplemented with 20% fructose. The fructose water was changed on a daily basis to avoid prolems associated with the fermentation process. [22].

Animals montoring

Changes in metaolic parameters were examined weekly in the animals (body weight, water uptake and total daily Calories uptake)[23].

The amount of rodent chow consumed and the amount of fructose consumed within 24 hours were used to calculate total calories consumed [24].

The Oral Glucose Tolerance Test (OGTT) was performed after 12 hrs of mice fasting along with the commencement and the end of the study. The bedding was changed before starting the fasting process to ensure absence of the bedding of any food particle [25].

Procedure of oral glucose tolerance test (OGTT):

12-hr fasted mice (with free accesss to water) were given 50 mg of glucose (2g/kg) for each, using gavage through a gastric tube, which was inserted orally to the stomach. At 0, 30, 60, 90, and 120 minutes after glucose loading, blood samples were obtained from the jugular vein using a lancet for venepuncture.The results were recorded [26].

In vivo biological evaluation of the synthesized compounds (OGTT):

After the process of animal model has been completed, 24 mice were taken (weighing 45-50 g) to be tested for *in vivo* biological activity of the synthesized compounds.The same procedure and circumstances were used for OGTT as mentioned above.

The 24 mice were divided into four experimental groups, each with six individuals. Groups; I and II received compounds; 1c and 2c respectively in a dose of (50 mg / kg) given orally [27], [28], [29]& [30]. Group III was considered as a negative control group that received vehicle only (5% DMSO) given orally, while group IV was considered as a positive control that received metformin in a dose of 30 mg / kg (p.o.).

Each of the four groups of mice received a glucose load (2g/kg) orally 30 minutes after receiving the drug via gastric tube. Blood samples were taken soon before the drug was administered, as well as 0, 30, 60, 90, and 120 minutes after glucose load. Blood sample collection was achieved by puncturing the jugular vein with a lancet and the blood was transferred with a capillary tube to be measured immediately by the glucometer device. Serum glucose levels were measured and recorded for each mouse [31],[32],[33].

Enzymatic activity evaluation of the synthesized compounds:

Blood samples were taken from each mouse in the four groups immediately after the last glucose level measurement was taken at the end of the OGTT. The blood samples (average volume ~ 1.0 ml/ mouse) for the 24 mice were collected in Eppendorf Tubes, assembled, and centrifuged to separate the serum, which will be used to measure GK activity by GK activity assay kit. After the completion of centrifugation process, serum samples were withdrawn using micropipette, collected again in Eppendorf Tubes, which would be coded and kept for the next step.

The reagents of the kit were warmed to room temperature, dissolved, and added to the 96-well microplate followed by the addition and mixing of the samples. The microplate then inserted into the microplate reader to be read at 340 nm and the absorbance was recorded at 20th and 320th second [27], [34] & [35]

Results and discussion
Structures docking

In silico computational docking studies were carried out using GOLD (Genetic Optimization of Ligand Docking), which was provided by the Cambridge Crystallographic Data Center (CCDC). Glucokinase enzyme (PDB ID: 5V4X) is the target protein. Compounds 1c and 2c were docked in the enzyme's allosteric binding site with various GOLD scores (based on their PLP fitness related to complex formation at the active site) and specifications, as stated in table (4) shown below.

_____

The docking of chemical structures including; binding site amino acid residues, hydrogen bonding, hydrophobic interaction, and lengths of bonds along with poses of these compounds at the allosteric activation site of the enzyme were shown in figures 3 to 6.

The best ligand bound complex (PDB ID: 5V4X) was selected after studying a number of entries and evaluating the three-dimensional structures with the highest resolution. The catalytic site of this enzyme incorporates a glucose molecule, while the allosteric site contains an activator molecule (8wj).

The compounds derived from the diazole-benzamide moiety were designed and synthesized depending on the analyses of GK activators described in previous studies in the literature binding to the allosteric region of GK. The drug-likeness features of these compounds like molecular weight, log P, hydrogen bond donors (HBD), and hydrogen bond acceptors (HBA) are provided in tables (5 and 6). The compounds chosen for in silico investigations were found to have drug-like characteristics according to Lipinski's rule of five.

GK's allosteric site is mainly comprised of residues from the large and small domains, as well as two loops that connect them, and it is widely known that all known GKAs bind here. [36].

This allosteric site comprises of Arg 63, Tyr 215, Met 210, Tyr 214, Val 452 and Val 455 residues [21]. At this site the synthesized compounds were docked. Docking scores which include; PLP fitness, H-bonding, and hydrophobic interactions as well as the amino acids concerned with these interactions, were listed in table (4).
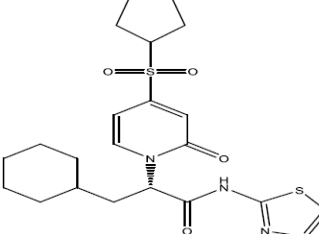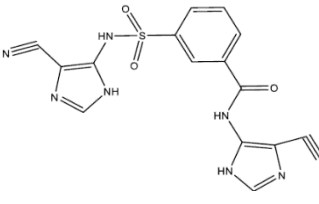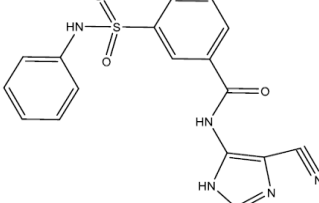
Compounds (1c & 2c) were analyzed in details depending on their higher PLP scores and docking interactions in the binding site (regarding number of H-bonding, hydrophobic interactions and lengths of these bonds).

Analyses of H-bond interactions

With a distance of 3.078 A°, the docked pose revealed an H-bond interaction between the 'N' of the diazole ring of compound 1c and the 'H' of the primary amine of Trp 99 on GK protein. (Fig. 3).

Compound 2c forms two H-bonds with GK, as shown in Fig. (5): one is between the 'N' of the sulfonamide group of compound 2c and the 'H' of the hydroxyl group of Arg 63 on GK protein, with a distance of 2.944 A°;, and the other is between the 'N' of cyano group of compound 2c and the 'H' of the phenolic hydroxyl group of Tyr 214 on GK protein with a distance of 2.904 A° .

Table (4): *In silico* design, No. of H-bonding, Amino acids included in H-bonding, Amino acids included in hydrophobic interactions, and Docking score (PLP fitness):

Comp	Structure	No. of H-bonding	Amino acids included in H-bonding	Amino acids included in hydrophobic interactions	Docking score (PLP fitness)
REF. Ligand (8wj)		3	TRP 99, TYR 214, ARG 63	TYR 214, TYR 215, TRP 99, ARG 63	121.75
1c		1	TRP 99	TRP 99, LEU 451, PRO 66, MET 210	72.77
2c		2	ARG 63, TYR 214	TYR 214, ARG 63, VAL 455, LYS 458	76.61

_____

Analyses of hydrophobic interactions

In addition to the H-bond forces, compound (1c & 2c) were bonded in the allosteric site by hydrophobic interactions made with hydrophobic pocket amino acid residues, which determine the pose of each compound in the binding site.

Compound 1c has hydrophobic interactions with Trp 99, Leu 451, Pro 66, and Met 210. while, compound 2c was observed to have hydrophobic interactions with Tyr 214, Arg 63, Val 455, and Lys 458.

By examining the H-bond and hydrophobic interactions of the best docked pose, compound 2c was found to have good binding in the allosteric region. Where this molecule has the same binding orientation as the co-crystallized ligand (8wj) in the allosteric site of the enzyme.

This was suggested by the pattern of H-bond and hydrophobic interactions with pocket comprising residues in addition to the higher value of PLP compared with compound 1c.
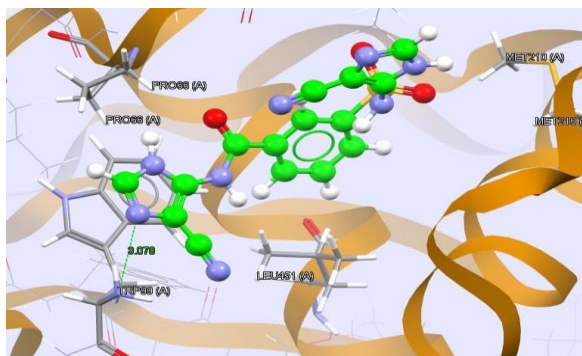
Figure (3): Crystal structure of compound 1c with GK (PDB entry: 5V4X). Amino acid residues included in H-bonding: TRP 99. [1c: Ball and stick shape, enzyme amino acid residues in a capped stick shape].
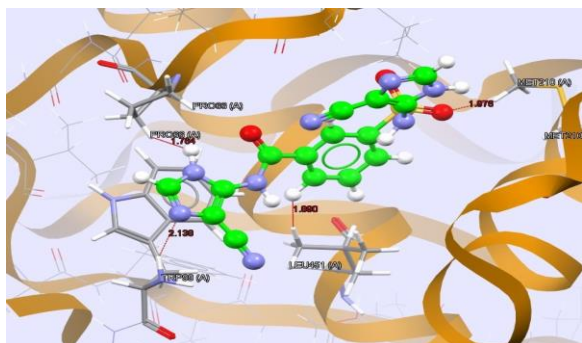
Figure (4): Crystal structure of compound 1c with GK (PDB entry: 5V4X). Amino acid included in hydrophobic interactions: TRP 99, LEU 451, PRO 66, MET 210.
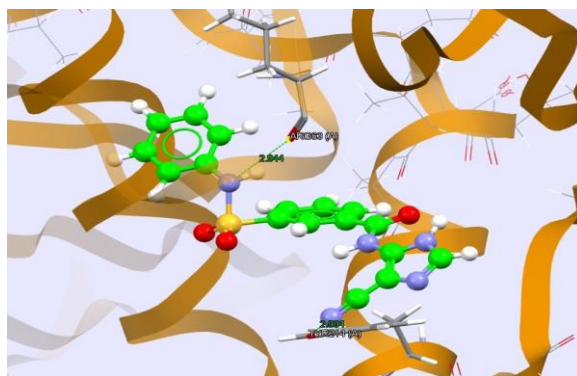
Figure (5): Crystal structure of compound 2c with GK (PDB entry: 5V4X). Amino acid residues included in H-bonding: ARG 63, TYR 214. [1c: Ball and stick shape, enzyme amino acid residues in a capped stick shape].
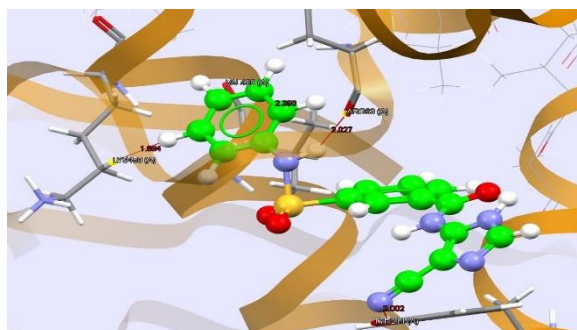

Figure (6): Crystal structure of compound 2c with GK (PDB entry: 5V4X). Amino acid included in hydrophobic interactions: TYR 214, ARG 63, VAL 455, LYS 458.

Results of chemical syntheses:

Tables (5) and (6) highlight the chemical and physical properties of the GKA derivatives that were successfully synthesized. The yield of the final products was relatively high. For all of the produced compounds, melting points were examined and reported. The Lipinski rule of five is very well accepted based on the predicted log P (n-octanol / water partition coefficient) parameters, H-bond donors, and H-bond acceptors [37] &[38].

However, the total no. of the rotatable bonds within the molecule is another important feature to the drug molecule for oral bioavailability. To be orally absorbable, the drug molecule should not have more than 10 rotatable bonds [39]. All the synthesized derivatives did not exceed this no. and obey this rule very well.

_____

Table (5) Physical properties of the synthesized compounds:

Comp	Physical appearance	Melting point (ºC)	Log P	tPSA*	Rf value	Water solubility
1c	Dark brown precipitate	98-100	0.39	188.59 Å²	0.49	2.68e-01 mg/ml Soluble
2c	Off-white precipitate	185-187	1.66	136.12 Å²	0.66	7.46e-02 mg/ml (Soluble)

*tPSA = The surface sum of all polar atoms of the molecules, namely oxygen and nitrogen, as well as their connected hydrogen atoms, is known as topological polar surface area

Table (6): Chemical properties of the synthesized compounds

Compound	Chemical formula	Molecular weight (g/mol)	Yield %	H-Bond Donor	H-Bond Acceptor	No. of rotatable bonds	No. of heavy atoms	No. of aromatic heavy atoms
1c	$C_{15}H_{10}N_8O_3S$	382.36	83	4	7	6	27	16
2c	$C_{17}H_{13}N_5O_3S$	367.38	89	3	5	6	26	17

Suggested mechanism of synthesis for compounds (1c & 2c):

Step 1: formation of sulphonamides:
Concisely, a nucleophilic attack of the aryl amine [the unshared pair of electrons on the nitrogen] to the corresponding electrophile [the partially positively charged sulfur of 3-(chlorosulfonyl) benzoic acid] to obtain the proposed sulphonamides as shown in scheme (2) bellow.
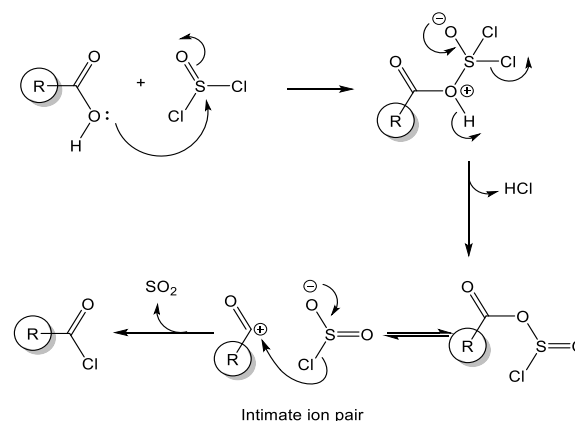
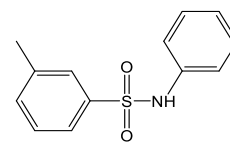Step 2: formation of benzoyl chlorides:
This stage involves producing benzoyl chlorides by refluxing the aforementioned products with thionyl chloride. It is also started with a nucleophilic attack of the carboxylic oxygen of the sulphonamide to their corresponding electrophilic sulfur of thionyl chloride and preceded in suggested mechanism illustrated in scheme (3) below.
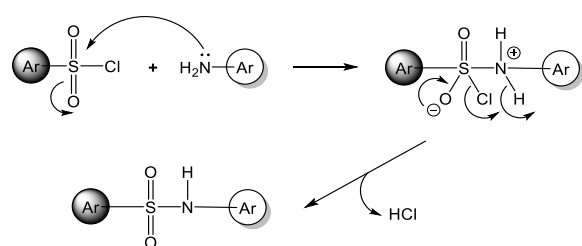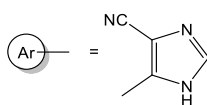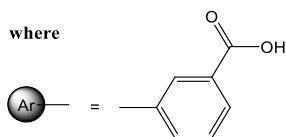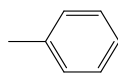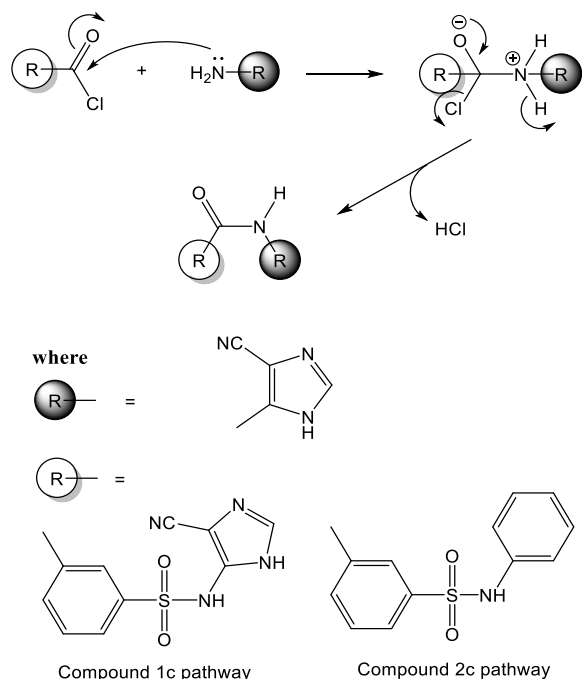

Scheme (2): Suggested mechanism of the formation of sulphonamides
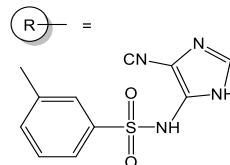
Scheme (3): Suggested mechanism of the formation of benzoyl chlorides

_____

Step 3: formation of diazole-benzamide derivatives:
It can be seen from scheme (4) below, the suggested mechanism of this step that started with the nucleophilic attack of the diazole amine to the corresponding electrophiles represented by the benzoyl chloride to synthesize the designed diazole-benzamide derivatives.

Scheme (4): Suggested mechanism the formation of diazole-benzamide derivatives

Results of characterization and identification of the synthesized compounds
FT-IR characterization: This mainly depends on the appearance or disappearance of specific bands through the IR spectra that correlate to the functional groups of the reactants or the products respectively.

FT-IR Characterization of compound (1c): 3423 cm-1 (N-H stretching vibration of sulfonamide), 3342 cm-1 (N-H stretching vibration of imidazole), 3132 cm-1 (N-H stretching vibration of amide), 2222 cm-1 (C≡N stretching vibration), 1645 cm-1 (C=O of amide), 1600 , 1558 & 1521 cm-1 ((C=N) & (C=C) aromatic stretching vibration overlap), 1379 & 1166 cm-1 (SO2 asymmetric & symmetric stretching vibration).

FT-IR Characterization of compound (2c): 3267 cm-1 (NH stretching vibration of sulfonamide), 3072 cm-1 (C-H aromatic stretching vibration), 1755 cm-1 (C=O of conjugated acid chloride), 1591 , 1519 & 1492 cm-1 (C=C aromatic stretching vibration), 1381 & 1153 cm-1 (SO2 asymmetric & symmetric stretching vibration).

^{1}H-NMR characterization:
^{1}H-NMR characterization and interpretation of compounds 1c and 2c are tabulated in tables 7 & 8 respectively. The spectra were recorded in DMSO-*d6* (deuterated dimethyl sulfoxide) solvent.

^{13}C NMR Characterization:
^{13}C-NMR characterization and interpretation of compounds 1c and 2c are tabulated in tables 9 & 10 respectively.

Table (7) ^{1}H NMR data and the interpretations of compound 1c:

Signal	Chemical shift (ppm)	No. of protons	Multiplicity	Interpretation
a	7.10-8.58	6H	Multiplet	Aromatic protons
b	10.74	1H	Singlet	Proton of secondary amine affected by neighboring carbonyl group and imidazole ring
c	11.25	1H	Singlet	Proton of secondary amine affected by neighboring SO$_2$ group and imidazole ring
d	12.32	2H	Singlet	Proton of secondary amine of imidazole ring (internal)

_____

_____

Table (8)^{1}H NMR data and the interpretations of compound 2c:

Signal	Chemical shift (ppm)	No. of protons	Multiplicity	Interpretation
a	7.07-8.65	10H	Multiplet	Aromatic protons
b	10.46	1H	Singlet	Proton of secondary amine affected by neighboring SO$_2$ group and benzene ring
c	10.86	1H	Singlet	Proton of secondary amine affected by neighboring carbonyl group and imidazole ring
d	11.78	1H	Singlet	Proton of secondary amine of imidazole ring (internal)

Table (9) ^{13}C NMR data and the interpretations of compound 1c:

Signal	Chemical shift (ppm)	No. of carbon atoms	Interpretation
a	113.29	2	(C─N) of imidazole ring
b	125.36	2	(C≡N) of cyanide group
c	126.46	1	Carbon of benzene ring
d	128.52	1	Carbon of benzene ring
e	129.55	1	Carbon of benzene ring
f	131.95	1	Carbon of benzene ring
g	143.06	1	Carbon of benzene ring adjacent to carbonyl group
h	148.32	2	(C=N) of imidazole ring
i	161.07	2	(C─NH) of imidazole ring adjacent to external amine
j	164.85	1	Carbon of benzene ring adjacent to SO$_2$ group
k	166.97	1	Carbon of carbonyl group

Mass Spectrometric Characterization:

Mass spectrometric methods were employed to detect and fully characterize the chemical compounds synthesized in this work. The mass spectra were recoded, the parent ions (m /z $^+$) were shown corresponding to the expected molecular mass of the compounds. Tables (11 & 12) summarized the fragmentation with the abundance and formula for each fragment.

_____

_____

Table (10) ^{13}C NMR data and the interpretations of compound 2c:

Signal	Chemical shift (ppm)	No. of carbon atoms	Interpretation
a	111.79	1	(C─N) of imidazole ring
b	120.70	1	(C≡N) of cyanide group
c	123.87	2	Carbon of benzene ring
d	125.21	1	Carbon of benzene ring
e	126.57	1	Carbon of benzene ring
f	129.79	3	Carbon of benzene ring
g	132.01	3	Carbon of benzene ring
h	135.96	1	Carbon of benzene ring adjacent to carbonyl group
i	137.98	1	(C═N) of imidazole ring
j	138.91	1	(C─NH) of imidazole ring adjacent to external amine
k	147.84	1	Carbon of benzene ring adjacent to SO$_2$ group
l	166.74	1	Carbon of carbonyl group

Animal model design (High fructose diet induced T2DM mouse)

The goal of this portion of the work was to develop a type II diabetes model in mice using a diet that was as similar to human intake as possible. This model would be used for biological assessment of the synthesized compounds to examine their antihyperglycemic activity [40].

Fructose has been used as a sweetener substitute (fructose corn syrup) which widely used recently in foods and beverages. This is considered as risk factor for obesity, dyslipidemia, insulin resistance, and heart disease. Excessive consumption of foods rich in sugar can trigger the onset of T2DM and metabolic disruption [41].

Animal models assist largely in the study of DM. These models enable researchers to manipulate factors that influence the progression of the disease and its consequences. [42].

Fructose, in short-term clinical trials, reduces insulin sensitivity and is usually used to induce metabolic syndrome, insulin resistance, and increased body mass [43].

As a result, the main goal was to create a reliable model that closely resembles the underlying pathophysiology of T2DM in humans, which is caused by persistent high-sugar consumption, in addition to genetic variables.

Glucose tolerance test used as a metabolic parameter to compare the results before and after the period of high-fructose diet applied for animals [44].

Our findings show that giving a 20 percent fructose solution to mice can enhance the development of T2DM easier and faster.

After 8 weeks of high fructose water ingestion, the test animals' metabolism changed, as evidenced by an increase in body weight and an upward shift in the glucose tolerance curve.

The following data represent the results of animal model design:
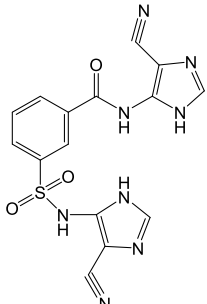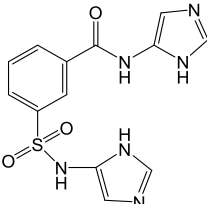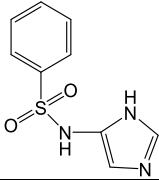
_____
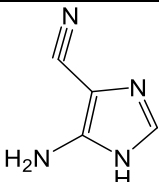
Table (11) Mass spectrometric data for compound 1c:
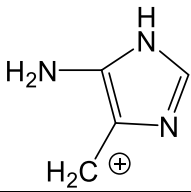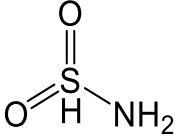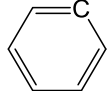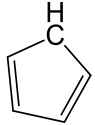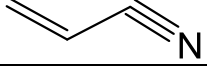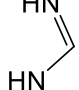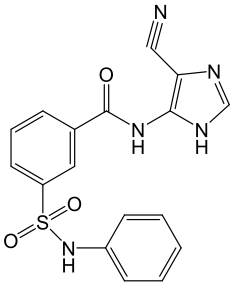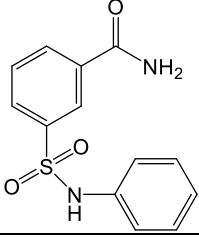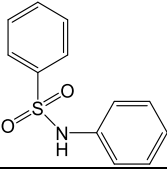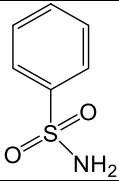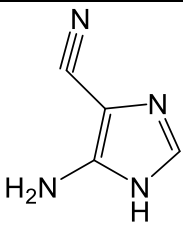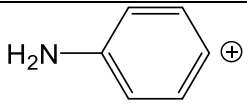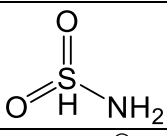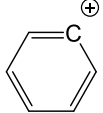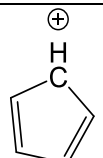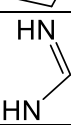
No.	Molecular mass	Chemical formula	Abundance	Structure
1	382	$C_{15}H_{10}N_8O_3S$	300000 Molecular ion	
2	332	$C_{13}H_{12}N_6O_3S$	400000	
3	223	$C_9H_9N_3O_2S$	1100000	
4	108	$C_4H_4N_4$	7900000 Base peak	
5	92	$C_4H_6N_3^+$	2000000	
6	81	H_3NO_2S	5000000	
7	77	C_6H_5	1800000	
8	65	C_5H_5	1300000	
9	53	C_3H_3N	6500000	
10	43	CH_3N_2	480000	

Table (12) Mass spectrometric data for compound 2c:

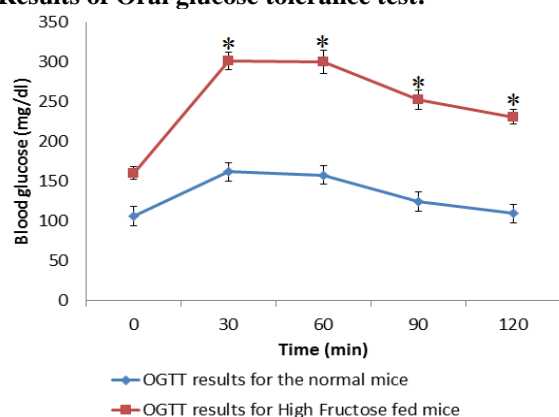| No.	Molecular mass	Chemical formula	Abundance	Structure
1	367	$C_{17}H_{13}N_5O_3S$	800000 Molecular ion	
2	276	$C_{13}H_{12}N_2O_3S$	460000	
3	233	$C_{12}H_{11}NO_2S$	1400000	
4	157	$C_6H_7NO_2S$	390000	
5	108	$C_4H_4N_4$	8400000 Base peak	
6	92	C_6H_7N	2100000	
7	81	H_3NO_2S	6000000	
8	77	C_6H_5	1000000	
9	65	C_5H_5	1500000	
10	43	CH_3N_2	490000	

_____

Results of Oral glucose tolerance test:

Figure (7): Average Oral glucose tolerance test for the 50 fasted 8-week old male mice (██), and OGTT results for the fasted mice after 8 weeks High

Fructose diet (██). Results were expressed as mean ±SD (* represents statistically significant difference with $p \leq 0.05$)
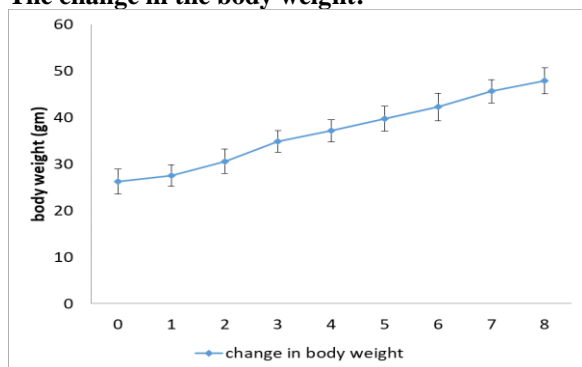
The change in the body weight:

Figure (8): High Fructose diet feeding induces obesity in mice: The average fasting body weight of 50 mice during the experimental period. Results were expressed as mean ±SD

The change in daily food intake:

Figure (9): Change in daily food intake: the average food intake of 50 mice, calculated as g/day/mouse, for 24 hr. at the end of each week during the experimental period.
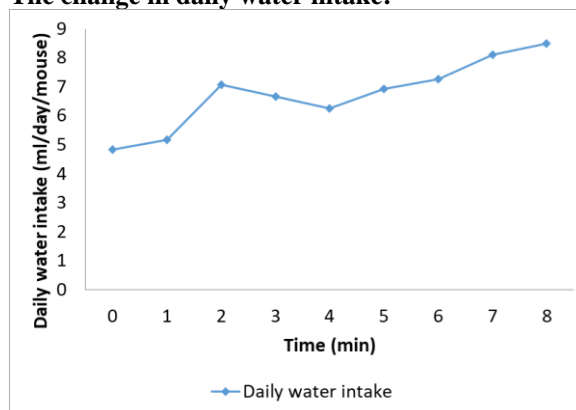
The change in daily water intake:

Figure (10): Change in daily water intake: the average water intake of 50 mice, calculated as ml/day/mouse, for 24 hr. at the end of each week during the experimental period.
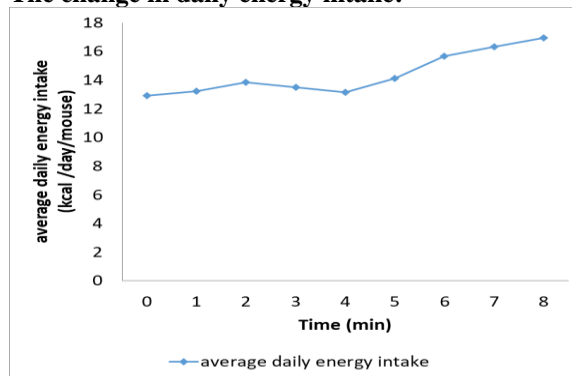
The change in daily energy intake:

Figure (11): Change in daily energy intake: the average energy intake of 50 mice, calculated as kcal/day/mouse, for 24 hr. at the end of each week during the experimental period.

From the above data, we can easily observe the impaired OGTT as well as the average weight was obviously increased after fructose treatment.

In addition to the significant shift in glucose tolerance curve, high fructose water administration resulted in alterations in glucose homeostasis, which were characterized by decreased food intake and an increase in water intake. This reflects the dependence of the animals on the fructose dissolved in the water as a source of energy more than the food, as a result average daily energy intake was increased ended with increased body weight and impaired OGTT.

Fructose consumption is proportional to the amount of water consumed by the animals, and their desire to consume regular rodent chow was reduced. As a result, these animals consumed a greater amount of fructose. In susceptible patients, this condition closely resembles the circumstance of ingesting a lot of fructose-rich drinks.

_____

In vivo biological evaluation of the synthesized compounds (OGTT):

The current work studied the hypoglycemic effect of a small molecule GKAs (diazole-benzamide derivatives) in a diet induced T2DM mouse model. An improved glycemia with varied degrees was achieved according to the results obtained from the OGTT test carried out for the synthsiezed compounds (1c & 2c) on the experimental animals. These results further support for the idea that GK can act a target for the treatment of T2DM [45].

The hypoglycemic effect of GK activation in mice fed a high fructose diet was investigated in this study. These mice developed impaired glucose tolerance after the period of modeling had been completed.

The antihyperglycemic activity of compounds 1c and 2c identified in the in silico study was evaluated further in animal models using the OGTT assay. Blood glucose levels (mg/dl) are measured at regular intervals to determine the effectiveness of antidiabetic therapy (-30, 0, 30, 60, 90, 120 minutes) as shown in figure (12) below.

By examining these results and the AUC for each compound as listed in table (13), compound 2c was found to have higher activity than compound 1c when compared to metformin as a reference therapy.

The results of hypoglycemic activity of the synthesized compounds indicated that changing the phenyl ring at sulphonamide nitrogen by other heterocyclic ring (cyano- imidazole ring) will greatly reduce hypoglycemic activity of the GKA
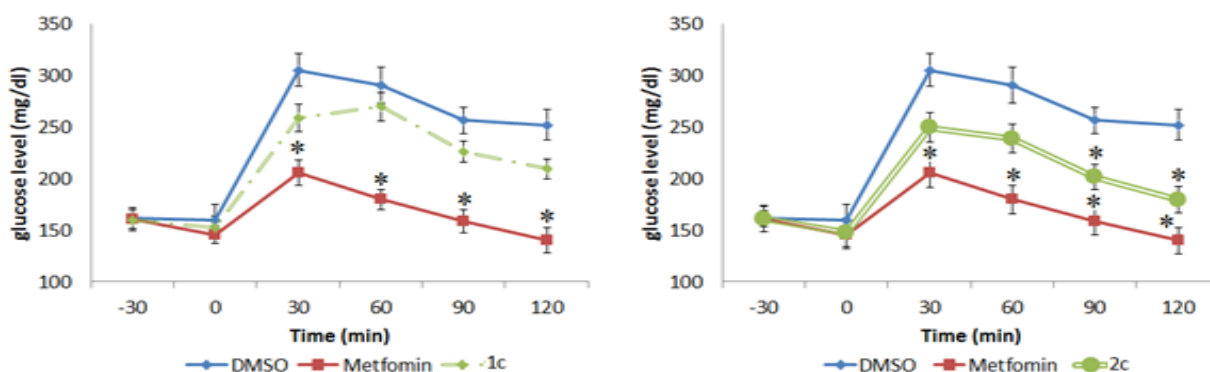
.

Figure (12): Effect of the synthesized compounds (1c & 2c) on blood glucose levels at specified time intervals in OGTT. All the values are mean of six measurements. (* represents statistically significant difference with $p \leq 0.05$). Results were expressed as mean $\pm$SD

Table (13): Area Under the Curve of DMSO, Metformin, Compound 1c, and 2c, as well as percent of change in AUC for the tested compounds as compared to the control:

Compound	Area Under the Curve (AUC)	Percent of change in AUC as compared to the control
DMSO	36,539 ± 2300	-
Metformin	25162 ±1458 *	31%
Compound 1c	32753±1695	10%
Compound 2c	30213±1752 *	17%

Enzymatic activity evaluation of the synthesized compounds:

The enzymatic GK activities were estimated spectrometrically for the synthesized compounds (1c & 2c) by a paired reaction with glucose-6-phosphate dehydrogenase enzyme using Hexokinase Microplate Assay Kit provided by MyBiosourse Company.

This technique simplifies the process of measuring GK activity directly in serum samples. A coupled

enzyme test is used to measure GK activity, in which a glucose molecule is phosphorylated by GK and transformed to G-6-P, which is subsequently oxidized by G-6-P dehydrogenase to generate NADPH, as follows:
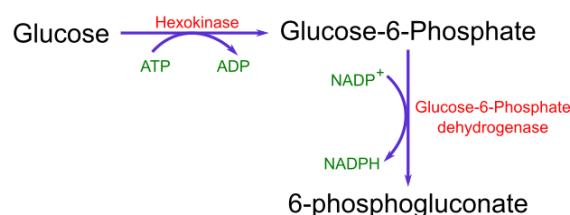
The resultant NADPH reduces a colorless probe that will result in a colorimetric product (at 340 nm), which is related to the amount of GK activity present [46]

The results of GK activation (fold activation) for the synthesized compounds along with metformin are listed in table (14). By comparing the fold activation of these compounds relative to DMSO as a negative control, we can easily observe the preference of

_____

compound 2c on compound 1c regarding their GK activation attitude.

It is clear that these results are consistent with that obtained from the OGTT study, which again support the important role of GK activation as a way to improve glucose homeostasis.

It is important to know that metformin, despite being more potent than other synthesized compounds as a hypoglycemic agent as noticed in OGTT results; it showed less GK activation than compounds; 1c and 2c. This is due to the multi mechanisms that metformin has as a hypoglycemic agent.

Table (14): Results of GK activity measurement using GK activity assay kit.

Compound	GK activity (Fold activation)
DMSO	1.00
Metformin	1.23
Compound 1c	1.08
Compound 2c	1.37

Conclusion

In present study, the authors conclude that novel diazole- benzamide derivatives as glucokinase activators were successfully designed, synthesized, and characterized. In silico docking studies showed that the designed compounds could form characteristic H-bonds with GK proteins in addition to the hydrophobic interaction. The present study investigated the activation of GK in high fructose fed mice with impaired glucose test. Compound 2c showed better antihyperglycemic activity than compound 1c and better GK activation in enzymatic assay. The results of the OGTT test were consistent with those of the enzymatic assay and in silico docking investigations.

Conflicts of interest

The authors affirm that the publishing of this research article does not include any conflicts of interest.

References:

[1] H. Chen, Q. Nie, J. Hu, X. Huang, W. Huang, and S. Nie, "Metabolism amelioration of Dendrobium officinale polysaccharide on type II diabetic rats," *Food Hydrocoll.*, vol. 102, p. 105582, 2020.

[2] A. Hazari and G. A. Maiya, "Epidemiology and current status of diabetes mellitus and diabetic foot syndrome," in *Clinical Biomechanics and its Implications on Diabetic Foot*, Springer, 2020, pp. 13–22.

[3] F. Anagnostou, "Pathway analysis of type 2 Diabetes Mellitus," 2021.

[4] Z. S. Cheruvallath *et al.*, "Discovery of potent and orally active 1,4-disubstituted indazoles as novel allosteric glucokinase activators," *Bioorganic Med. Chem. Lett.*, vol. 27, no. 12, pp. 2678–2682, 2017, doi: 10.1016/j.bmcl.2017.04.041.

[5] A. S. Grewal, V. Lather, N. Charaya, N. Sharma, S. Singh, and V. Kairys, "Recent developments in medicinal chemistry of allosteric activators of human glucokinase for type 2 diabetes mellitus therapeutics," *Curr. Pharm. Des.*, vol. 26, no. 21, pp. 2510–2552, 2020.

[6] D. Patidar, A. Jain, P. K. Mohanty, and V. Asati, "NOVEL MULTI ACTION THERAPY APPROACHES OF GLUCOKINASE ACTIVATOR TO TREAT TYPE 2 DIABETES.," *J. Adv. Sci. Res.*, vol. 11, no. 3, 2020.

[7] S. Kalra, A. G. Unnikrishnan, M. P. Baruah, R. Sahay, and G. Bantwal, "Metabolic and Energy Imbalance in Dysglycemia-Based Chronic Disease," *Diabetes, Metab. Syndr. Obes. Targets Ther.*, vol. 14, p. 165, 2021.

[8] P. Sharma, S. Singh, V. Thakur, N. Sharma, and A. S. Grewal, "Novel and emerging therapeutic drug targets for management of type 2 Diabetes Mellitus," *Obes. Med.*, p. 100329, 2021.

[9] R. Jayaraman, S. Subramani, S. H. S. Abdullah, and M. Udaiyar, "Antihyperglycemic effect of hesperetin, a citrus flavonoid, extenuates hyperglycemia and exploring the potential role in antioxidant and antihyperlipidemic in streptozotocin-induced diabetic rats," *Biomed. Pharmacother.*, vol. 97, pp. 98–106, 2018.

[10] J. E. Campbell and C. B. Newgard, "Mechanisms controlling pancreatic islet cell function in insulin secretion," *Nat. Rev. Mol. cell Biol.*, vol. 22, no. 2, pp. 142–158, 2021.

[11] J. Zhang and F. Liu, "The De-, Re-, and trans-differentiation of β-cells: Regulation and function," in *Seminars in cell & developmental biology*, 2020, vol. 103, pp. 68–75.

[12] A. B. Engin and A. Engin, "Protein Kinases Signaling in Pancreatic Beta-cells Death and Type 2 Diabetes," in *Protein Kinase-mediated Decisions Between Life and Death*, Springer, 2021, pp. 195–227.

[13] A. J. Scheen, "New hope for glucokinase activators in type 2 diabetes?," *Lancet*

Diabetes Endocrinol., vol. 6, no. 8, pp. 591–593, 2018.

[14]   S. Singh, S. Arora, E. Dhalio, N. Sharma, K. Arora, and A. S. Grewal, "Design and synthesis of newer N-benzimidazol-2yl benzamide analogues as allosteric activators of human glucokinase," *Med. Chem. Res.*, vol. 30, no. 3, pp. 760–770, 2021.

[15]   A. S. Grewa, N. Sharma, and S. Singh, "Molecular docking investigation of compounds from sapium ellipticum (Hochst) pax as allosteric activators of human glucokinase," *Int. J. Pharm. Qual. Assur.*, vol. 10, no. 04, pp. 571–577, 2019.

[16]   W. Yu and A. D. MacKerell, "Computer-aided drug design methods," in *Antibiotics*, Springer, 2017, pp. 85–106.

[17]   A. Lee and D. Kim, "CRDS: consensus reverse docking system for target fishing," *Bioinformatics*, vol. 36, no. 3, pp. 959–960, 2020.

[18]   A. S. Grewal, R. Kharb, D. N. Prasad, J. S. Dua, and V. Lather, "Design, synthesis and evaluation of novel 3, 5-disubstituted benzamide derivatives as allosteric glucokinase activators," *BMC Chem.*, vol. 13, no. 1, pp. 1–14, 2019.

[19]   K. Vandyck *et al.*, "Synthesis and evaluation of N-phenyl-3-sulfamoyl-benzamide derivatives as capsid assembly modulators inhibiting hepatitis B virus (HBV)," *J. Med. Chem.*, vol. 61, no. 14, pp. 6247–6260, 2018.

[20]   P. E. Wall, *Thin-layer chromatography: a modern practical approach*. Royal Society of Chemistry, 2007.

[21]   N. Charaya, D. Pandita, A. S. Grewal, and V. Lather, "Design, synthesis and biological evaluation of novel thiazol-2-yl benzamide derivatives as glucokinase activators," *Comput. Biol. Chem.*, vol. 73, pp. 221–229, 2018.

[22]   Z. O. Ibraheem, R. Basir, A. K. Aljobory, O. E. Ibrahim, A. Alsumaidaee, and M. F. Yam, "Impact of gentamicin coadministration along with high fructose feeding on progression of renal failure and metabolic syndrome in Sprague-Dawley rats," *Biomed Res. Int.*, vol. 2014, 2014.

[23]   K. Sayehmiri, I. Ahmadi, and E. Anvari, "Fructose feeding and hyperuricemia: A systematic review and meta-analysis," *Clin. Nutr. Res.*, vol. 9, no. 2, p. 122, 2020.

[24]   S. Rivière *et al.*, "High fructose diet inducing diabetes rapidly impacts olfactory epithelium and behavior in mice," *Sci. Rep.*, vol. 6, no. 1, pp. 1–13, 2016.

[25]   M. H. Abdulla, M. A. Sattar, and E. J. Johns, "The relation between fructose-induced metabolic syndrome and altered renal haemodynamic and excretory function in the rat," *Int. J. Nephrol.*, vol. 2011, 2011.

[26]   J. E. Ayala *et al.*, "Standard operating procedures for describing and performing metabolic tests of glucose homeostasis in mice," *Dis. Model. Mech.*, vol. 3, no. 9–10, pp. 525–534, 2010.

[27]   J. Grimsby *et al.*, "Allosteric activators of glucokinase: potential role in diabetes therapy," *Science (80-.).*, vol. 301, no. 5631, pp. 370–373, 2003.

[28]   F. M. Matschinsky *et al.*, "Research and development of glucokinase activators for diabetes therapy: theoretical and practical aspects," *Diabetes-Perspectives Drug Ther.*, pp. 357–401, 2011.

[29]   M. S. Winzell *et al.*, "Chronic glucokinase activation reduces glycaemia and improves glucose tolerance in high-fat diet fed mice," *Eur. J. Pharmacol.*, vol. 663, no. 1–3, pp. 80–86, 2011.

[30]   N.-E. Haynes *et al.*, "Discovery, structure–activity relationships, pharmacokinetics, and efficacy of glucokinase activator (2 R)-3-cyclopentyl-2-(4-methanesulfonylphenyl)-N-thiazol-2-yl-propionamide (RO0281675)," *J. Med. Chem.*, vol. 53, no. 9, pp. 3618–3625, 2010.

[31]   A. J. F. King, "The use of animal models in diabetes research," *Br. J. Pharmacol.*, vol. 166, no. 3, pp. 877–894, 2012.

[32]   N. Charaya, D. Pandita, A. S. Grewal, and V. Lather, "Design, synthesis and biological evaluation of novel thiazol-2-yl benzamide derivatives as glucokinase activators," *Comput. Biol. Chem.*, vol. 73, pp. 221–229, 2018, doi: 10.1016/j.compbiolchem.2018.02.018.

[33]   C.-Y. Wang and J. K. Liao, "A mouse model of diet-induced obesity and insulin resistance," in *mTOR*, Springer, 2012, pp. 421–433.

[34]   L. S. Bertram *et al.*, "SAR, pharmacokinetics, safety, and efficacy of glucokinase activating 2-(4-sulfonylphenyl)-N-thiazol-2-ylacetamides: discovery of PSN-GK1," *J. Med. Chem.*, vol. 51, no. 14, pp. 4340–4345, 2008.

[35]   L. Zhang *et al.*, "Benzamide derivatives as dual-action hypoglycemic agents that inhibit glycogen phosphorylase and activate glucokinase," *Bioorg. Med. Chem.*, vol. 17, no. 20, pp. 7301–7312, 2009.

[36]   S. Liu *et al.*, "Insights into mechanism of glucokinase activation: observation of multiple distinct protein conformations," *J. Biol. Chem.*, vol. 287, no. 17, pp. 13598–

13610, 2012.

[37] P. Patnaik, *Dean's analytical chemistry handbook*. McGraw-Hill Education, 2004.

[38] P. D. Leeson and B. Springthorpe, "The influence of drug-like concepts on decision-making in medicinal chemistry," *Nat. Rev. Drug Discov.*, vol. 6, no. 11, pp. 881–890, 2007.

[39] M. Á. Cabrera-Pérez and H. Pham-The, "Computational modeling of human oral bioavailability: what will be next?," *Expert Opin. Drug Discov.*, vol. 13, no. 6, pp. 509–521, 2018.

[40] C.-C. Chyau *et al.*, "Antrodan alleviates high-fat and high-fructose diet-induced fatty liver disease in C57BL/6 mice model via AMPK/Sirt1/SREBP-1c/PPARγ pathway," *Int. J. Mol. Sci.*, vol. 21, no. 1, p. 360, 2020.

[41] V. S. Malik and F. B. Hu, "Sugar-sweetened beverages and cardiometabolic health: an update of the evidence," *Nutrients*, vol. 11, no. 8, p. 1840, 2019.

[42] R. D. Wilson and M. S. Islam, "Fructose-fed streptozotocin-injected rat: an alternative model for type 2 diabetes," *Pharmacol. reports*, vol. 64, no. 1, pp. 129–139, 2012.

[43] J. Dupas *et al.*, "Progressive induction of type 2 diabetes: effects of a reality–like fructose enriched diet in young Wistar rats," *PLoS One*, vol. 11, no. 1, p. e0146821, 2016.

[44] J. Dupas *et al.*, "Progressive induction of type 2 diabetes: Effects of a reality-like fructose enriched diet in young Wistar rats," *PLoS One*, vol. 11, no. 1, pp. 1–13, 2016, doi: 10.1371/journal.pone.0146821.

[45] M. Coghlan and B. Leighton, "Glucokinase activators in diabetes management," *Expert Opin. Investig. Drugs*, vol. 17, no. 2, pp. 145–167, 2008.

[46] F. Li, Q. Zhu, Y. Zhang, Y. Feng, Y. Leng, and A. Zhang, "Design, synthesis, and pharmacological evaluation of N-(4-mono and 4, 5-disubstituted thiazol-2-yl)-2-aryl-3-(tetrahydro-2H-pyran-4-yl) propanamides as glucokinase activators," *Bioorg. Med. Chem.*, vol. 18, no. 11, pp. 3875–3884, 2010.